Talanta 85 (2011) 1310–1316

Contents lists available at ScienceDirect

Talanta

journal homepage: www.elsevier.com/locate/talanta

Continuous flow method for the simultaneous determination of phosphate/arsenate based on their different kinetic characteristics

Laura Borgnino[a,b], Valeria Pfaffen[b], Pedro J. Depetris[a], Miriam Palomeque[a,*]

[a] CICTERRA, Universidad Nacional de Córdoba, Ciudad Universitaria, 5000, Córdoba, Argentina
[b] INFIQC, Universidad Nacional de Córdoba, Ciudad Universitaria, 5000, Córdoba, Argentina

ARTICLE INFO

Article history:
Received 1 February 2011
Received in revised form 27 May 2011
Accepted 1 June 2011
Available online 12 June 2011

Keywords:
Arsenate
Phosphate
Stopped-flow
Spectrophotometry

ABSTRACT

This paper proposes a new automated spectrophotometric method for the simultaneous determination of phosphate and arsenate without pre-treatment, which is faster, simpler, less expensive and hazardous than other well-known methods used with water samples. Such method is based on the different kinetic characteristics of complex formation of phosphate and arsenate with ammonium molybdate. A flow system was used in order to achieve good mixing and to provide precise time control. All the measurements were performed at the isosbestic point wavelength (885 nm). Chemical variables were optimized by factorial design (ammonium molybdate 0.015 mol L^{-1}, potassium antimony tartrate 1×10^{-4} mol L^{-1}, and sulphuric acid 0.7 mol L^{-1}). An appropriate linear range for both analytes (0.50–8.00 μmol L^{-1}), good inter-day reproducibility (4.9% [P] and 3.3% [P + As]) and a sample throughput of 6 h^{-1} were obtained. The detection limits are 0.4 μmol L^{-1} P and 0.19 μmol L^{-1} [P + As] (3.3 Sy/x). The method was validated.

1. Introduction

Arsenic and phosphorus are very important in aquatic geochemistry and sediment–water interface sciences because they are usually involved in processes related to water contamination. Phosphorus is an essential nutrient for the aquatic biota and limits its primary productivity [1]. Although it is not toxic, an overload accelerates eutrophication [2] and impairs water quality [1]. Phosphorus is released into the aquatic environment mainly by anthropogenic sources (industrial, agricultural, and mining activities). Arsenic, on the other hand, is not only toxic but also carcinogenic, and both natural and anthropogenic sources are responsible for high levels of it which contaminate the environment [3,4]. It can be found in food, water, and air in organic and inorganic form [5] and it can exist in several oxidation states (−3, 0, +3 and +5) [6–8]. Inorganic arsenic species occur as arsenite and arsenate, the former being much more toxic [6] and predominant under anaerobic (reducing) conditions, while arsenate is stable under aerobic (oxidizing) conditions [3,7]. In recent years, many countries (e.g. China, Chile, Bangladesh, Taiwan, Mexico, Argentina, Poland, Canada, Hungary, Japan, and India) have reported high concentrations of arsenate in water, soil and sediments [7,9]. Long-term consumption of drinking water contaminated with arsenate is a major threat to human health since it has been reported to cause skin, lung, kidney, and liver cancer [3,6].

Although food, which mainly contains organic forms of arsenate, is the main source of arsenate exposure, its toxicity in drinking water is more significant due to the high levels of inorganic species that can be present. The US EPA regulation requires the concentration of inorganic arsenate in drinking water to be below 10 μg L^{-1}, which demands more accurate and sensitive analytical techniques. So far, hydride generation atomic absorption spectrophotometry (HG-AAS), inductively-coupled plasma (ICP), graphite furnace (ETAAS), and ICP mass spectrometry (MS) are the most accurate laboratory instrumentation suitable for arsenate measurement in water, with detection limits that could well satisfy the US EPA requirements. However, this instrumentation is very expensive and not always available in routine laboratories. On the other hand, the colorimetric molybdenum blue method (standard method) is simple and only requires a photometer, but it is not suitable for the determination of arsenate at trace levels. Thus, there is a pressing need for affordable, simple methods with low limits of detection in order to determine arsenate at low level concentrations in accordance with stringent EPA requirements.

The molybdenum blue method is well-established for determining inorganic arsenate and phosphate in solution, and it has been broadly used [10]. However, arsenate determination by this method has the disadvantage of requiring around 1 h for color development of the arsenate–molybdate complex. Furthermore, arsenate/phosphate mixtures cannot be quantified simultaneously because both species exhibit the same behavior and interfere with each other. For this reason, several modifications of the

* Corresponding author at: FCEFyN UNC, Av Vélez Sarsfield 1611, 5016, Córdoba, Argentina. Tel.: +54 351 4693555; fax: +54 351 4334139.
E-mail addresses: mirpalom@efn.uncor.edu, mirpalom@hotmail.com (M. Palomeque).

0039-9140/$ – see front matter © 2011 Elsevier B.V. All rights reserved.
doi:10.1016/j.talanta.2011.06.001

molybdenum blue method have been reported in recent years. Linge and Oldham [11] have optimized quantification of phosphate/arsenate mixtures by adding a reducing agent (i.e. sodium sulphite) in order to eliminate arsenate interference in concentrations above 100 μg L^{-1}. Despite the fact that the method was improved by such addition, this step requires about 1½ h for completion of the reaction and color development. A detailed discussion of virtually all modifications to the molybdenum blue method reported in the literature has been provided by Tsang et al. [12], who in turn proposed a new modification for fast and accurate measurement of arsenate/phosphate mixtures. It consisted in using sodium dithionite as reducing agent, which reduced color development time. However, a complete reduction of arsenate only occurs after heating the solution at 80 °C for 20 min, and then cooling it to room temperature before applying spectrophotometric detection. Lopez Carreto et al. [13] determined arsenate/phosphate simultaneously via the kinetic wavelength-pair method, with arsenate concentration exceeding that of phosphate. The method proposed by Abbas [14] allows determination of both species in the presence of each other. It is based on the adsorption of arsenomolybdic and phosphomolybdic acids on polyurethane sorbent varying the pH of the sample. It requires the preparation of the sorbent material, time-consuming for the step of separation and high volume of sample. On the other hand, Ramírez Cordero and Cañizares Macías [15] developed a sequential injection analysis (SIA) method for determining As(V), As(III) and P(V) in mixtures based on different reaction temperatures. It requires six calibration curves to determine the analytes simultaneously.

Flow analysis offers significant advantages in terms of precision and accuracy for time control and it allows data acquisition from reaction kinetics by using the stopped-flow mode. The aim of this study is to present the automated method for simultaneous quantification of phosphate/arsenate in water samples without pre-treatment and with a minimum time consumption for the overall analytical process, which we have developed taking advantage of the significant difference between complex-formation kinetics of phosphate and arsenate.

2. Experimental

2.1. Apparatus

A UV–vis spectrophotometer (Shimadzu UV-VIS 1700) with a Hellma 178-010 QS flow cell (inner volume 32 μL) was used to quantify phosphate and arsenate solutions.

The propulsion system was a Gilson Minipuls 3 peristaltic pump, and a Rheodyne 5041 injection valve was used as selection valve. All reaction coils were made of PTFE tubing (inner diameter 0.5 mm).

The determination of phosphate and arsenate in real samples was carried out by an external laboratory. Ion chromatography (IC) with carbonate eluent anion exchange column (ionPac As22) and suppressed conductivity detection [19,20] and ICP-MS [21–23] were used as reference methods.

STATISTICA statistical software packages were used for data treatment [24].

2.2. Reagents and solutions

Reagents: Sulphuric acid (Carlo Erba, As^V < 0.000001%), ascorbic acid (Anedra, $C_6H_8O_6$), ammonium molybdate $(NH_4)_6Mo_7O_{24}{\cdot}4H_2O$ (Tetrahedron), potassium antimony tartrate $(K(SbO)C_4H_4O_6){\cdot}2H_2O$ (Anedra), $Na_2HAsO_4{\cdot}7H_2O$ (Anedra), and NaH_2PO_4 (Baker), were used as received to prepare the solutions.

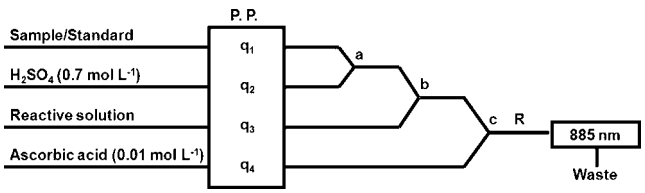

Fig. 1. P.P.: Peristaltic pump, q: flow rates. Reactive solution: ammonium molybdate (0.015 mol L^{-1}), potassium antimony tartrate (1×10^{-4} mol L^{-1}), and sulphuric acid (0.7 mol L^{-1}); q_1: 1.79 mL min^{-1}, q_2: 0.37 mL min^{-1}, q_3: 1.09 mL min^{-1}, q_4: 0.79 mL min^{-1}; R: coiled reactor (1 m), a, b, c: confluence points.

All solutions were prepared using analytical reagent-grade chemicals and ultra pure water of Milli-Q quality (18.0 mΩ cm^{-1}).

A stock solution of arsenate was prepared by dissolving 0.0156 g of $Na_2HAsO_4{\cdot}7H_2O$ with water to make up to 50 mL. To prepare a *phosphate stock solution* 0.0069 g of $NaH_2PO_4{\cdot}H_2O$ was dissolved in 50 mL of water. Both stock solutions were 1000 μmol L^{-1}. The calibration solutions were prepared by diluting the stock solutions with water.

A solution of ammonium molybdate (0.1 mol L^{-1}) was prepared by weighing 6.1793 g $(NH_4)_6Mo_7O_{24}{\cdot}4H_2O$ and adding water up to 50 mL.

A tartrate solution (0.01 mol L^{-1}) was prepared by dissolving 0.0835 g of $K(SbO)C_4H_4O_6{\cdot}2H_2O$ with 25 mL of water

A sulphuric acid solution (4 mol L^{-1}) was prepared by taking 11.11 mL of sulphuric acid (δ = 1.835 g/cm^3) and diluting it with water up to 50 mL.

The reactant solution was prepared by mixing 15 mL of ammonium molybdate solution, 1 mL of tartrate solution, and 17.5 mL of sulphuric acid with pure water up to 100 mL.

A solution of *ascorbic acid* (0.02 mol L^{-1}) was prepared by dissolving 0.352 g with water and making up to 100 mL.

3. Experimental design

Factorial design was employed to reduce the total number of experiments in order to achieve the best overall optimization of the process [25]. Since this method provides greater precision in the estimation of the overall main factor effects and its interactions, it is a powerful tool for simultaneous optimization of several variables. A common experimental design is one with all input factors set at each of two levels. These levels are called 'high' and 'low' or '+1' and '−1', respectively. If there are two levels for each k factor, a full factorial design has 2^k runs. In the present study, a two-level, full factorial design for three factors (2^3 runs) was used for modeling the optimization of chemical variables.

4. Procedure

The optimized continuous flow system that we have developed is shown in Fig. 1. Reagents are introduced into the system with a peristaltic pump (PP). The sample stream (q_1: 1.79 mL min^{-1}) converges with a sulphuric acid stream (0.7 mol L^{-1}; q_2: 0.37 mL min^{-1}). The resulting mixture first meets a stream of a 'reactive solution' (ammonium molybdate 0.015 mol L^{-1} + antimony tartrate 1.0×10^{-4} mol L^{-1} + sulphuric acid 0.7 mol L^{-1}; q_3: 1.09 mL min^{-1}) and then an ascorbic acid stream (0.01 mol L^{-1}; q_4: 0.79 mL min^{-1}). Finally, the mixture passes through a reactor (R: 100 cm) and the signal is measured at λ = 885 nm. After a fixed time (15–20 s) during which the baseline is established, the flow is stopped and kinetic curves are obtained.

In order to obtain the calibration curves, each phosphate standard solution is measured up to a constant signal (approximately 200 s). Then, the flow is restored and the next standard solution is introduced into the system. Data at 100 s are used to obtain the

Table 1
Factorial design matrix for three variables and experimental absorbance values.

Experiment	Replicate	A	B	C	Absorbance	λ (nm)[a]
1	1	−1	−1	−1	0.116	833
2	1	+1	−1	−1	0.118	841
3	1	−1	+1	−1	0.000	–
4	1	+1	+1	−1	0.000	–
5	1	−1	−1	+1	0.081	830
6	1	+1	−1	+1	0.000	–
7	1	−1	+1	+1	0.124	866
8	1	+1	+1	+1	0.128	888
9	2	−1	−1	−1	0.110	833
10	2	+1	−1	−1	0.115	841
11	2	−1	+1	−1	0.000	–
12	2	+1	+1	−1	0.000	–
13	2	−1	−1	+1	0.084	830
14	2	+1	−1	+1	0.000	–
15	2	−1	+1	+1	0.127	866
16	2	+1	+1	+1	0.130	888

The experiments were randomly performed.
[a] Isosbestic point wavelengths.

individual phosphate (P) calibration curve, while data at a maximum absorbance value are considered for phosphate plus arsenate (P + As).

When real samples are introduced into the system, the signal is measured for more than 600 s after stopping the flow (see Section 5.4), because this is the minimum time needed to obtain a complete color development for the molybdoarsenate complex. Thus, the absorbance measured at 100 s and that measured after reaching constant value are considered for determining P and (P + As), respectively, by using the corresponding calibration curves.

5. Results and discussion

The proposed method was based on the formation of molybdoarsenate and molybdophosphate complexes, taking into account their kinetic characteristics. Our interest was the development of an automated system for simultaneous determination of both chemical species, without sample pre-treatment and with minimum time consumption.

5.1. Selection of flow manifold

Configuration of the flow injection system was tested using a phosphate standard solution since phosphate has a reaction rate higher than that of arsenate. In this case, a standard volume was injected into a sulphuric acid carrier solution. After mixing, this solution merged first with a stream of reactant solution in a reactor, and then with ascorbic acid in a second reactor, where the complex was formed. Different sample volumes, flow rates, and reactor lengths were analyzed, but no signal improvement was observed.

Best reproducibility, enhanced signal intensity, and a lower limit of detection were attained with a continuous flow system design, as shown in Fig. 1. By using this system, an appropriate and reproducible time control was achieved, allowing the stopped-flow mode to be applied. Bearing in mind that the sample is continuously introduced, the system was designed to maintain the order of reagent addition reported as optimal in a previous work [12]. The optimization of chemical variables was carried out under these conditions (see below).

5.2. Influence of chemical and hydrodynamic variables

Phosphate and arsenate have similar physical and chemical properties. They are usually found together in water, phosphate commonly occurring at higher concentrations than arsenate. Besides, both anions can develop molybdophosphate and molybdoarsenate complexes with similar characteristics, but different complex-formation kinetics (i.e. under the same experimental conditions [12,16], the kinetics of phosphate complex-formation is faster than that of arsenate). In the developed procedure, the concentration of reagents involved in the 'reactive solution' has a significant dependence on their concentration ratio and on arsenate and phosphate concentration in solution, so they will have an influence on the color development rate, the stability of the complexes, etc. Their concentrations, as well as that of the other reagents in the system, were optimized together using chemometric tools. The study was first carried out by applying a 2^4 factorial design [24] which considered the following factors: ascorbic acid, ammonium molybdate, potassium antimony tartrate, and sulphuric acid concentration. The ascorbic acid concentration did not have any significant effect on color development, as previously reported

Table 2
Analysis of variance for absorbance with Table 1 data.

Factor	Sum of squares (SS)	Degrees of freedom (d.f.)	Mean squares (MS)	*F* ratio	*p* level[a]
A	0.001482	1	0.001482	2964.50	0.000
B	0.000992	1	0.000992	1984.50	0.000
C	0.002500	1	0.002500	5000.00	0.000
A × B	0.001681	1	0.001681	3362.00	0.000
A × C	0.001640	1	0.001640	3280.50	0.000
B × C	0.040602	1	0.040602	81204.50	0.000
A × B × C	0.001849	1	0.001849	3698.00	0.000
Error	0.000004	8	0.000001		0.000
Total SS	0.050751	15			0.000

[a] Significant factor at $p < 0.05$.

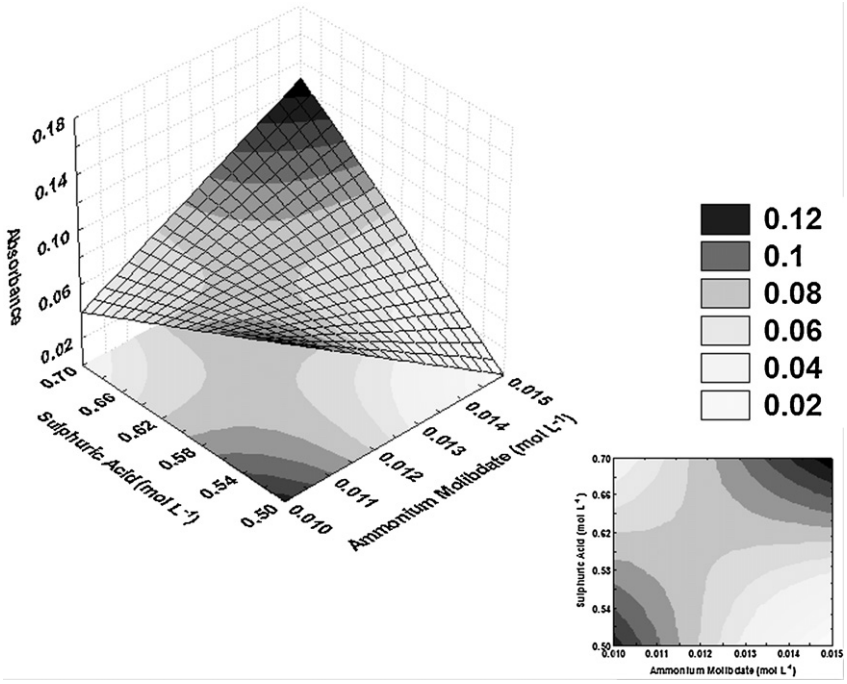

Fig. 2. 3D and 2D plot of the response surface for the most significant chemical parameters estimated using 2^3 full factorial design.

[16]. Hence, an intermediate concentration from the tested range (0.01 mol L^{-1}) was selected and eliminated as a factor before testing a new factorial design. Then, a 2^3 factorial design was applied, and spectrometric curves for both complexes (molybdophosphate and molybdoarsenate) were obtained under different experimental conditions. After achieving stability at different concentrations, both complexes have the same absorptivity; therefore, the isosbestic point was chosen to perform the absorbance measurements. Experimental values corresponding to high- and low-level reagent concentration were studied: potassium antimony tartrate (A), 0.8×10^{-4} mol L^{-1} (−1) and 1.2×10^{-4} mol L^{-1} (+1); ammonium molybdate (B), 0.010 mol L^{-1} (−1) and 0.015 mol L^{-1} (+1); sulphuric acid (C), 0.05 mol L^{-1} (−1) and 0.70 mol L^{-1} (+1). The factorial design results are shown in Table 1. Zero absorbance point is set when polymerization/coagulation of molybdenum complexes starts (appearance of a precipitate and excessive increase in the absorbance values as a function of time). This was observed in experiments 3, 4, 11, 12 (low level for sulphuric acid and high level for ammonium molybdate factors) and 6, 14 (high levels for sulphuric acid and potassium antimony tartrate with low level for ammonium molybdate factors). Analysis of the effects significance in a two-level factorial design was performed by an ANOVA test. The obtained results are presented in Table 2, where it can be observed that all factors and their interactions were significant ($p < 0.05$). However, the most significant factor influencing the response is the interaction B × C (molybdate–sulphuric acid). The R^2 value of 0.9999 indicate that almost 100% of the response variability could be explained by the model.

The interaction effect (magnitude and direction) between the two most important parameters is shown in a 3D surface response (Fig. 2). These results are in good agreement with previously reported ones. When the concentration of sulphuric acid is too high, complex formation becomes slower, while if it is too low complex stability diminishes [17]. A blue residue precipitates which is thought to result from polymerization/coagulation of the molybdate complexes. If the molybdate concentration is too high, the precipitate appears and the linear dependence of absorbance on analyte concentration is lost [18]. Stability of the molybdate complexes depends on the ratio between acid and molybdate concentration in the final solution [12,17]. It has been proved that low concentrations of both molybdate and sulphuric acid allow obtaining good signals, though these are highly variable due to low stability of the complex. Then, the optimum values were 0.7 mol L^{-1} for sulphuric acid, and 0.015 mol L^{-1} for ammonium molybdate. The effect of antimony tartrate concentration, on the other hand, was insignificant. However, a decrease in it has been reported to improve stability of both complexes though a concomitant decrease in the color development rate is observed [12]. An antimony tartrate concentration of 1.0×10^{-4} mol L^{-1} was therefore selected.

The effect of solution heating on the formation of molybdophosphate and molybdoarsenate complexes was also tested. Different temperatures in the 50–80 °C range were analyzed by immersing the reactor R into a thermostatic bath. Since heating of the solution leads to decomposition of the complexes, as reported in the literature [10,26] room temperature was used.

Once the chemical variables were optimized, analysis of the hydrodynamic ones was carried out by the univariant method. This procedure was performed in order to both improve mixing of reagent streams and minimize the stop-flow time. The range of variables studied as well as their optimum values are listed in Table 3. Large variations in flow variables around the original values produced significant changes in the reagent concentration ratio and the appearance of a precipitate. Thus, using the selected conditions, the working wavelength was 885 nm (Fig. 3 – inset).

Table 3
Studied range of flow variables and their optimum values.

Variable	Studied variable range	Optimum value of variable
q_1 (mL min^{-1})	1.00–2.00	1.79
q_2 (mL min^{-1})	0.2–1.00	0.37
q_3 (mL min^{-1})	0.5–1.50	1.09
q_4 (mL min^{-1})	0.5–1.00	0.79
R (cm)	50–200	100
Reactor a-b (cm)	1.0–10	2.0
Reactor b-c (cm)	1.0–10	2.0

Table 4
Effect of possible interferents on the signal of total concentration for P + As (2.5 μmol L^{-1}).

Interferent	Amount (mg L^{-1})	Error %
Na^+	150	4.2
K^+	146	2.3
Ca^{2+}	120	2.7
Mg^{2+}	30	1.7
Cr^{6+}	0.2	4.2
Cl^-	230	−3.9
F^-	2	1.6
SO_4^{2-}	300	2.5
NO_3^-	1	−2.0
NO_2^-	0.3	−3.1
Si	25	4.8

Table 5
Comparison of slopes at 100 s.

Samples	Slopes of standard addition method calibration	$\lvert t_{\text{calculated value}} \rvert$
A	0.00436 ± 0.00002	0.95
B	0.00376 ± 0.00036	0.47
C	0.00355 ± 0.00063	0.81
D	0.00395 ± 0.00028	0.00
E	0.00382 ± 0.00155	0.00

Slope of the calibration curve at 100 s: 0.00392 (±0.00010); $t(4,\alpha = 5\%) = 2.776$.

5.3. Kinetic characteristics of the complex-formation reactions

Using the above-mentioned operational conditions, it was observed that phosphate develops the molybdophosphate complex significantly faster than arsenate, as previously reported [12,16]. For this reason, absorbance vs. time curves from different analyte concentrations were carried out, beginning from the moment when the flow system is stopped (Fig. 3). As it can be seen, the molybdophosphate complex reaches signal stability at approximately 200 s, while the molybdoarsenate complex does so at above 600 s. In both cases, the maximum signal reached at the same analyte concentration has the same absorbance value. This fact allowed calibration curves to be obtained using only phosphate standards for the determination of both analytes.

5.4. Analytical application

In order to eliminate the interference of arsenate in phosphate determination, some reducing agents were used to pre-treat the sample. Since this resulted in a very tedious and time-consuming procedure, we decided to perform a simultaneous determination of both analytes without sample pre-treatment, taking advantage of the significant differences in the complex-formation kinetics and considering reproducible time control with flow systems.

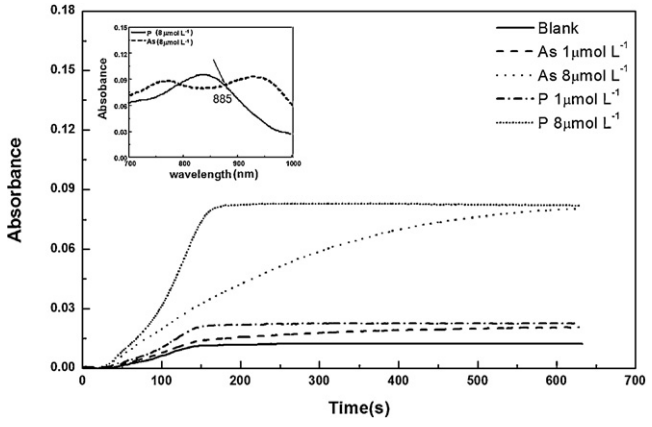

Fig. 3. Kinetic curves from: blank (grey line), As 1 μmol L^{-1} (dotted line), As 8 μmol L^{-1} (black line), P 1 μmol L^{-1} (dash-dot line) and P 8 μmol L^{-1} (dashed grey line).

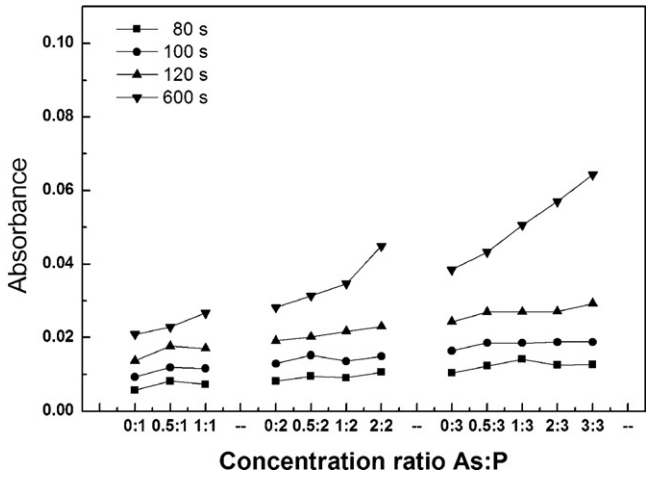

Fig. 4. Absorbance values of solutions measured at different times and As:P concentration ratios (P concentrations: 1, 2, and 3 μmol L^{-1}) and under optimum experimental conditions.

The difference between both signals depends on the concentration ratio between the analytes. While the molybdophosphate complex formation is detected from the moment when the system flow is stopped, the molybdoarsenate complex signal begins to be significant at 120 s, in relation to the molybdophosphate complex signal at the same time. For this reason, kinetic curves were performed according to the above-mentioned procedure, and absorbance values at 80, 100, 120 and 600 s were obtained. Solutions at three different phosphate concentrations (1, 2 and 3 μmol L^{-1}) and increasing concentrations of arsenate on each one were prepared. Fig. 4 depicts the absorbance vs. concentration ratio curves. From the comparison between them, it is clear that data corresponding to 80 and 100 s are constant for all the As:P ratios studied. On the other hand, an increment in the signal is observed at 120 and 600 s as arsenate concentration increases. Then, phosphate could well be determined until 100 s without arsenate interfer-

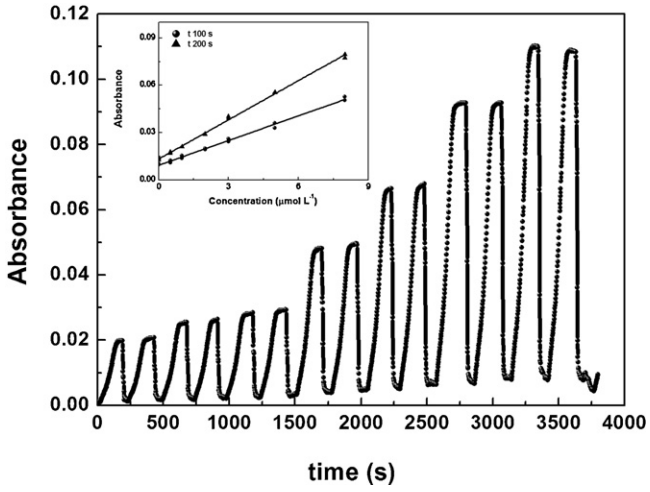

Fig. 5. Kinetic curves obtained by using the flow system proposed (standard concentrations: 0.5; 1.0; 2.0; 3.0; 5.0; and 8.0 μmol L^{-1}) in order to obtain the calibration curves. *Inset*: calibration curves obtained by using measurements from the kinetic curves at 100 s and 200 s.

Table 6
Comparison of slopes at 600 s.

Samples	Slopes of standard addition method calibration	$\lvert t_{calculated\ value} \rvert$
A	0.00774 ± 0.00181	0.26
B	0.00782 ± 0.00140	0.33
C	0.00726 ± 0.00118	0.58
D	0.00759 ± 0.00079	0.00
E	0.00798 ± 0.00002	0.11

Slope of the calibration curve at 600 s: 0.00758 (±0.00011); $t(4,\alpha = 5\%) = 2.776$.

ence, thus maximizing analytical sensitivity and minimizing error in phosphate quantification. Phosphate concentration in nature is generally higher than that of arsenate; then, the latter would not interfere in phosphate determination at 100 s.

The calibration curves for P and P + As were obtained using phosphate standards at different concentration values. Kinetic curves for each standard were recorded until the signal was constant (Fig. 5). The linear range for simultaneous determination of P and As was 0.50–8.00 μmol L^{-1}. The calibration curve at 100 s was $A = 0.0039_2$ ($\pm 0.0001_3$) [μmol L^{-1} X] + 0.0050_5 ($\pm 0.0005_2$), $n = 12$, $R^2 = 0.996$, detection limit (LOD) = 0.4 μmol L^{-1} (3.3 Sy/x), allowing only P determination. When the signal was constant, the calibration curve was $A = 0.0075_8$ ($\pm 0.0001_1$) [μmol L^{-1} X] + 0.0143_1 ($\pm 0.0004_3$), $n = 12$, $R^2 = 0.999$ with a LOD of 0.19 μmol L^{-1} (3.3 Sy/x) allowing determination of the total P + As content. The inter-day reproducibility (RSD %) was estimated by running six independent calibration curves under different conditions (standard solution, reagent solution, etc.) on different days. The mean slopes were 0.0039_2 ($\pm 0.0001_9$) [RSD = 4.9%], and 0.0076_3 ($\pm 0.0002_6$) [RSD = 3.3%], respectively ($n = 6$ calibration curves) and a sample throughput of 6 h^{-1} was obtained.

5.5. Validation and application to real samples

The effect of ions commonly present in natural water samples was evaluated. No interference was found (relative error < 5% on the signal) for 1.5 μmol L^{-1} P + 1.0 μmol L^{-1} As standards over a total concentration of P + As [μmol L^{-1}] (Table 4).

Matrix interferences can be evaluated by comparing the slopes for the standard addition curve on real samples with the calibration curve. If the matrix does not interfere, both lines must have the same slope. For standard addition, potable water and river water samples filtered with a 0.45 μm-filter to remove particulate matter were used. The total dissolved solids (TDS) were less than 3000 mg L^{-1} for all the samples used, depending on their origin. Tables 5 and 6 show the slopes obtained for 5 standard addition curves for different samples (A–E) at 100 and 600 s, respectively. The slopes were compared with the calibration curve slope by the "*t*" test [27] and no statistical differences were found ($t_{calculate\ value} < t_{(4,\alpha = 0.05)}$), indicating the absence of a matrix effect.

Table 7
P and As determination in real samples. Study of recovery using the same samples.

Sample[a]	Amount (μmol L^{-1})					
	Added	Found ± SD[b]				
	(P + As)	Proposed method			Reference methods	
		100 s (P)	600 s (P + As)	As	Phosphorus[c]	Arsenic[d]
A	0	0.52 ± 0.04	0.58 ± 0.03	n.d.	n.d.	0.13
B	0	0.51 ± 0.04	0.51 ± 0.02	n.d.	n.d.	0.11
C	0	0.55 ± 0.06	0.58 ± 0.04	n.d.	n.d.	0.09
D	0	0.58 ± 0.06	0.60 ± 0.01	n.d.	n.d.	0.06
E-I	0	n.d.	n.d.	n.d.	n.d.	<0.02
J	0	3.01 ± 0.03	5.27 ± 0.01	2.26	n.d.	2.32
K	0	1.73 ± 0.04	2.94 ± 0.03	1.21	n.d.	1.14
	Amount (μmol L^{-1})					
	Added	Recovery ± SD[b]			Recovery %	
	(P + As)	100 s	600 s		P	As
A	1.50 + 1.02	1.55 ± 0.08	2.47 ± 0.02		103.3	92.1
B	1.50 + 1.02	1.43 ± 0.09	2.40 ± 0.03		95.3	95.1
C	1.50 + 1.02	1.56 ± 0.06	2.54 ± 0.03		104.0	96.1
D	1.50 + 1.02	1.50 ± 0.07	2.40 ± 0.04		100.0	88.2
E	1.50 + 1.02	1.52 ± 0.08	2.53 ± 0.01		101.3	98.0
F	1.50 + 1.02	1.51 ± 0.09	2.54 ± 0.02		100.6	101.0
J	1.00 + 1.02	0.96 ± 0.08	2.02 ± 0.00		96.0	103.9
K	1.50 + 1.02	1.46 ± 0.05	2.49 ± 0.01		97.3	100.1
A	2.50 + 1.53	2.38 ± 0.04	4.06 ± 0.01		95.2	112.0
B	2.50 + 1.53	2.58 ± 0.06	3.99 ± 0.00		103.2	92.2
C	2.50 + 1.53	2.32 ± 0.07	3.80 ± 0.04		92.8	98.7
D	2.50 + 1.53	2.50 ± 0.05	4.07 ± 0.03		100.0	104.7
E	2.50 + 1.53	2.48 ± 0.03	3.96 ± 0.01		99.2	98.7
K	2.50 + 1.53	2.52 ± 0.03	4.10 ± 0.00		100.8	97.4
B	3.00 + 1.02	2.90 ± 0.04	3.90 ± 0.01		96.7	98.0
C	3.00 + 1.02	2.83 ± 0.05	3.93 ± 0.00		94.3	107.8
G	3.00 + 1.02	2.96 ± 0.04	4.01 ± 0.02		98.7	102.9
H	3.00 + 1.02	3.20 ± 0.06	4.19 ± 0.00		106.7	97.0
I	3.00 + 1.02	3.10 ± 0.05	4.19 ± 0.01		103.3	106.8

[a] A–D: well water samples from different points of the city of Cordoba, E–I: river water; J: well water sample from the city of Bahía Blanca and K: well water sample from the city of Coronel Pringles, both samples from the province of Buenos Aires, Argentina.
[b] Standard deviation $n = 3$; n.d.: not detected.
[c] Results by using IC (P: LOD 150 μg $L^{-1} \sim 4.7$ μmol L^{-1}).
[d] Values obtained by using ICP-MS (As: LOD 0.03 μg $L^{-1} \sim 4 \times 10^{-4}$ μmol L^{-1}).

The results obtained via the developed method were compared with those obtained in an external laboratory (methods used: IC (for phosphate determination) and ICP-MS (for arsenate determination) (Table 7). It can be observed that, in these samples, phosphate could not be determined by using the reference method because its concentration was below the corresponding detection limit. Samples A–D showed the same signals at 100 s and at 600 s, indicating that only phosphate could be determined in them by the proposed method. Moreover, samples E–I, did not show significant signals for both analytes. For samples A–I, though arsenate concentration was below the detection limit, it could not be determined by the developed method. This is consistent with the results obtained via the reference method for arsenate determination. However, both phosphate and arsenate were detected in samples J and K, and the arsenic concentration agrees with that obtained by the reference method.

On the other hand, the same samples were spiked and the recovery percentages were obtained (Table 7) which were satisfactory indicating that the proposed method is appropriate to be applied to these kinds of samples.

For the above-exposed findings, the recovery percentages and the standard addition method allowed discarding proportional systematic errors, and therefore the accuracy of this methodology was proved.

6. Conclusions

In relation to other methodology for the measurement of phosphate/arsenate mixtures cited in the literature [10–14], the method proposed in the present work offers some significant advantages. It is readily applicable to natural water samples and it is faster and simpler, since no pre-treatment is necessary before the formation of the colored complex with ammonium molybdate. Thus, the time of the total analytical process is minimized. Besides, it has good sensitivity and reproducibility since the detection limit was improved as compared with other flow methodology [15]. Its precision and linear range is appropriate for phosphate and arsenate determination in natural water samples. Finally, its very low reagent consumption and minimal waste make it more affordable and less hazardous than other known methods. Because of all these features we can definitely propose it as quite a convenient method for the simultaneous determination of phosphate and arsenate.

Acknowledgements

The authors wish to acknowledge CONICET and SeCyT-UNC for financial support. L.B. and P.D. are members of CICyT in Argentinaĭs CONICET. VP thanks CONICET for the scholarships granted. We are especially grateful to P.I. Ortiz for her helpful suggestions which improved this manuscript. Language assistance by translator Ms. Karina Plasencia is gratefully acknowledged.

References

[1] R. Pourriot, M. Meybeck, Limnologie Générale, Masson, Paris, 1995.
[2] J. Hilton, M. O'Hare, M.J. Bowes, J.I. Jones, Sci. Total Environ. 365 (2006) 66.
[3] United States Environmental Protection Agency, UESPA, 1999, Doc. EPA 815-P-01-001.
[4] D. Mohan, C.U. Pittmant, J. Hazard. Mater. 142 (2007) 1.
[5] P.L. Smedley, D.G. Kinniburgh, Appl. Geochem. 17 (2001) 517.
[6] L. Ebdon, L. Pitts, R. Cornelis, H. Crews, O.F.X. Donard, Ph. Quevauviller (Eds.), Trace Element Speciation For Environmental, Food and Health, Royal Society of Chemistry, Cambridge, 2001.
[7] B.K. Mandaland, K.T. Suzuki, Talanta 58 (2002) 201.
[8] World Health Organization, Guidelines for Drinking-water Quality [electronic resource]: Incorporating First Addendum, vol.1, Recommendations, third ed., 2006.
[9] J.D. Paoloni, M.E. Sequeira, C.E. Fiorentino, J. Environ. Health 67 (2005) 50.
[10] V. Lenoble, V. Deluchat, B. Serpaud, J.-C. Bollinger, Talanta 61 (2003) 267.
[11] K.L. Linge, C.E. Oldham, Anal. Chim. Acta 450 (2001) 247.
[12] S. Tsang, F. Phu, M.M. Baum, G.A. Poskrebyshev, Talanta 71 (2007) 1560.
[13] Lopez Carreto, D. Sicilia, S. Rubio, D. Perez-Bendito, Anal. Chim. Acta 283 (1993) 481.
[14] M.N.D. Abbas, Anal. Lett. 36 (2003) 1231.
[15] B.E. Ramírez Cordero, M.P. Cañizares Macías, Talanta (2009) 1069.
[16] S. Blomqvist, K. Hjellstrom, A. Sjosten, Int. J. Environ. Anal. Chem. 54 (1993) 31.
[17] R.E. Stauffer, Anal. Chem. 55 (1983) 1205.
[18] T. Liu, E. Diemann, H. Li, A.W.M. Dress, A. Muller, Nature 426 (2003) 59.
[19] V. Ruiz-Calero, M.T. Galceran, Talanta 66 (2005) 376.
[20] K. Dash, S. Thangavel, S.V. Rao, K. Chandrasekaran, S.C. Chaurasia, J. Arunachalam, J. Chromatogr. A 1036 (2004) 223.
[21] M. Gerboles, D. Buzica, R.J.C. Brown, R.E. Yardley, A. Hanus-Illnar, M. Salfinger, B. Vallant, E. Adriaenssens, N. Claeys, E. Roekens, K. Sega, J. Jurasovic, S. Rychlik, E. Rabinak, G. Tanet, R. Passarella, V. Pedroni, V. Karlsson, L. Alleman, U. Pfeffer, D. Gladtke, A. Olschewski, B. O'Leary, M. O'Dwyer, D. Pockeviciute, J. Biel-Cwikowska, J. Tursic, Atmos. Environ. 45 (2011) 3488.
[22] E.J. Llorent-Martínez, P. Ortega-Barrales, M.L. Fernández-De Córdova, A. Domínguez-Vidal, A. Ruiz-Medina, Food Chem. 127 (2011) 1257.
[23] Z. Fiket, N. Mikac, G. Kniewald, Food Chem. 126 (2011) 941.
[24] Statistica V. 6, StatSoft, Tulsa, USA, 2001.
[25] D.C. Montgomery, Design and Analysis of Experiments, third ed., Wiley and Sons, 1991.
[26] A. Sjosten, S. Blomqvist, Water Res. 31 (1997) 1818.
[27] D.L. Massart, B.G.M. Vandeginste, L.M.C. Buydens, S. De Jong, P.J. Lewi, J. Smeyers-Verbeke, Handbook of Chemometrics and Qualimetrics, Part A, Elsevier, Amsterdam, 1997.